

π^-p Interactions at 905, 960, and 1100 MeV*

E. PICKUP,† D. K. ROBINSON, E. O. SALANT, F. AYER, AND B. A. MUNIR‡

Brookhaven National Laboratory, Upton, New York

(Received 18 June 1963)

Single-pion production in π^-p interactions has been studied at 905, 960, and 1100 MeV. Comparison with the isobar and one-pion-exchange (OPE) mechanisms of pion production shows that, below 1 BeV, pion production occurs primarily through the formation of an intermediate excited state of the nucleon (isobar), while at higher energies the influence of the ρ resonance in the $\pi\pi$ system becomes increasingly important. There is some evidence for an $I=2$ state in the events at the lower energies.

I. INTRODUCTION

SEVERAL groups have reported work on various aspects of pion production in π^-p and π^+p interactions near 1 BeV in hydrogen bubble chambers. In π^-p collisions at 960 MeV, Alles-Borelli *et al.*¹ showed the dominance of the $\frac{3}{2}, \frac{3}{2}$ pion-nucleon isobar in accord with the model of Lindenbaum and Sternheimer.² The work of Derado and Schmitz³ at 1 BeV indicated deviations from this model, and showed the influence of peripheral collisions in single-pion production. Work from Brookhaven⁴ and from the Cavendish Laboratory⁵ at 960 MeV also showed the importance of peripheral collisions and indicated the possible existence of a resonance in the $\pi\pi$ system. The existence of an $I=1$, $J=1^+$ resonance (ρ) in the $\pi\pi$ system at a mass of 750 MeV with width of 120 MeV has been established by the work of several groups.⁶⁻⁸

This paper gives results of the analyses of two-pronged events at 905, 960, and 1100 MeV. Of particular interest is the single-pion production which is compared with predictions of the isobar and one-pion-exchange models. The effects of the ρ resonance are also considered. Some preliminary results of these experiments have been reported previously.^{4,9}

II. TECHNICAL DETAILS

The bubble chamber pictures used in the present experiments were obtained from three sources.

* Work performed under the auspices of the U. S. Atomic Energy Commission.

† Present address: Rutherford High Energy Laboratory, Chilton, Didcot, Berks, England.

‡ Present address: Ohio University, Athens, Ohio.

¹ F. Alles-Borelli, S. Bergia, E. Perey Ferreira, and P. Waloschek, *Nuovo Cimento* **14**, 211 (1959).

² S. J. Lindenbaum and R. M. Sternheimer, *Phys. Rev.* **105**, 1874 (1957); R. M. Sternheimer and S. J. Lindenbaum, *Phys. Rev.* **109**, 1723 (1958).

³ I. Derado and N. Schmitz, *Phys. Rev.* **118**, 309 (1960).

⁴ E. Pickup, F. Ayer, and E. O. Salant, *Phys. Rev. Letters* **5**, 161 (1960).

⁵ J. G. Rushbrooke and D. Radojicic, *Phys. Rev. Letters* **5**, 567 (1960).

⁶ A. R. Erwin, R. March, W. D. Walker, and E. West, *Phys. Rev. Letters* **6**, 628 (1961).

⁷ D. Stonehill, C. Baltay, H. Courant, W. Fickinger, E. C. Fowler, H. Kraybill, J. Sandweiss, J. Sanford, and H. Taft, *Phys. Rev. Letters* **6**, 624 (1961).

⁸ E. Pickup, D. K. Robinson, and E. O. Salant, *Phys. Rev. Letters* **7**, 192 (1961).

⁹ B. A. Munir, E. Pickup, D. K. Robinson, and E. O. Salant, *Phys. Rev. Letters* **6**, 192 (1961).

(1) 905 MeV. These exposures were taken in the BNL 20-in. hydrogen bubble chamber at the Cosmotron in the pion beam used in the cusp experiment.¹⁰ 1285 two-pronged events were measured on digitized microscopes. Track reconstruction was made with the TRED computer program, and the events were fitted by the GUTS program to the single-pion production types

$$\pi^- + p \rightarrow \pi^- + \pi^+ + n, \quad (1)$$

$$\pi^- + p \rightarrow \pi^- + \pi^0 + p, \quad (2)$$

and to elastic scattering

$$\pi^- + p \rightarrow \pi^- + p. \quad (3)$$

The average measured error in momentum was about 3%.

(2) 960 MeV. These pictures were obtained from an exposure made at the Cosmotron by Eisler *et al.*¹¹ to study strange particle production in the Columbia 12-in. hydrogen bubble chamber. 1600 two-pronged interactions were measured. These were in a central region of the bubble chamber, chosen to give reasonably long secondary tracks, and to minimize track distortion which was present in some pictures. Track curvatures were measured on the film with templates and with digitized microscopes, and a least-squares fit was made. This information was then used to make a graphical event reconstruction. The average error in momentum was 5-10%. The accuracy in angle determination was $\sim \frac{1}{2}^\circ$.

(3) 1100 MeV. These pictures were obtained from Berkeley¹² and were taken in the 10-in. hydrogen bubble chamber. 1593 two-pronged events in a central fiducial volume were measured on digitized microscopes. Track reconstruction was made by the HYDRO computer program, and event fitting was done by the GUTS program. The measuring error was about 10% in momentum.

Since there was some possibility of kinematic am-

¹⁰ L. Bertanza, P. L. Connolly, B. B. Culwick, F. R. Eisler, T. Morris, R. Palmer, A. Prodel, and N. P. Samios, *Phys. Rev. Letters* **8**, 332 (1962).

¹¹ F. R. Eisler, R. Plano, A. Prodel, N. Samios, M. Schwartz, J. Steinberger, P. Bassi, V. Borelli, G. Puppi, H. Tanaka, P. Waloschek, V. Zoboli, M. Conversi, P. Franzini, I. Mannelli, R. Santangelo, and V. Silvestrini, *Nuovo Cimento* **10**, 468 (1958).

¹² We wish to thank Dr. Alvarez and his group for the loan of these pictures.

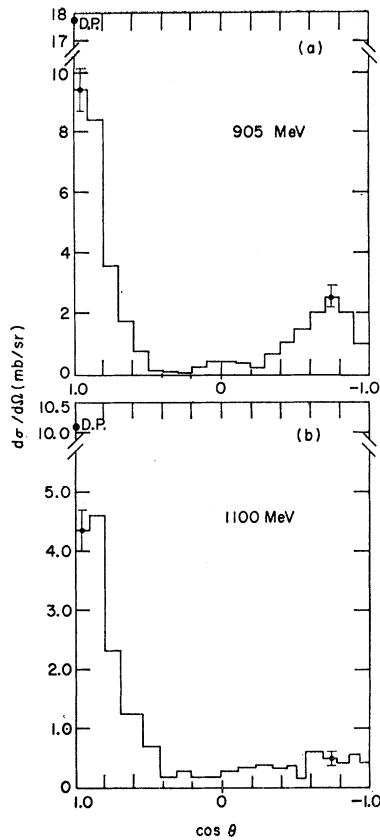


FIG. 1. Differential cross sections for π - p elastic scattering at (a) 905 MeV and (b) 1100 MeV. The points marked D. P. are obtained from the dispersion calculation of Cronin (See Ref. 15).

biguities in classifying reactions, because of finite measuring errors, all positive secondary particles were identified by ionization density. Events which did not fit one of the three reactions were classified as multiple-pion production (involving π^0 's). Further details of our analysis procedure may be found in Fickinger *et al.*¹³

TABLE I. Partial cross sections in mb.

	905 MeV	1100 MeV
Elastic scattering	25.1 ± 3.0	14.6 ± 0.8
$p\pi^-\pi^0$	6.5 ± 0.5	4.3 ± 0.3
$n\pi^-\pi^+$	10.7 ± 0.6	7.3 ± 0.6
$p\pi^+$ +neutrals ^a	0.2 ± 0.1	0.8 ± 0.1
$\pi^-\pi^+$ +neutrals ^b	0.8 ± 0.2	3.1 ± 0.5
Nonstrange neutrals ^c	11.9 ± 1.1	5.4 ± 0.3
Four prongs	0.6 ± 0.1	0.7 ± 0.1
Strange particles ^d	<0.1	0.7 ± 0.1
Total	55.9	36.9

^a $\pi^-\pi^+\pi^0 \rightarrow \pi^-\pi^+\pi^0$ +(2 or more neutral particles).

^b $\pi^-\pi^+\pi^0 \rightarrow \pi^-\pi^+\pi^0$ +(2 or more neutral particles).

^c Corrected for Λ^0 and Σ^0 modes.

^d From J. Steinberger, in *Proceedings of the 1958 Annual International Conference on High-Energy Physics at CERN* (CERN, Geneva, 1958), p. 147.

¹³ W. J. Fickinger, E. Pickup, D. K. Robinson, and E. O. Salant, *Phys. Rev.* **125**, 2082 (1962).

III. PARTIAL CROSS SECTIONS AND ELASTIC SCATTERING

For the 905- and 1100-MeV experiments all events were recorded (including stopping tracks, four-pronged stars, and strange particle events). The sums of the partial cross sections were normalized to the total cross sections from counter measurements reported by Devlin *et al.*¹⁴ At 1100 MeV absolute cross sections were also determined by counting beam tracks in the pictures; the total cross section obtained in this way was 34.8 ± 1.4 mb, to be compared with the counter value of 36.9 ± 0.9 mb. At 960 MeV picture quality and beam intensity were variable so that no cross sections were obtained.

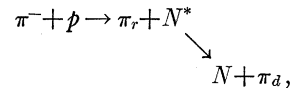
Partial cross sections are listed in Table I. Corrections have been applied for small-angle scanning losses in the elastic scattering, and for overlap between the χ^2 distributions for the different event interpretations. The errors include the uncertainty in these corrections as well as the statistical errors.

Figure 1 shows the differential elastic scattering angular distributions for 905 and 1100 MeV. The scanning losses at small angles were obtained by extrapolation to the point at 0° given by the dispersion calculations of Cronin.¹⁵ The distributions are similar to those obtained by Wood *et al.*¹⁶ for this energy region.

IV. SINGLE-PION PRODUCTION

A. Pion Momentum Distributions and the Isobar Model

Pion scattering experiments¹⁷ have shown the existence of resonances in the π - p system at total c.m. energies of 1230 MeV ($I=\frac{3}{2}, J=\frac{3}{2}$), 1520 MeV ($I=\frac{1}{2}, J=\frac{3}{2}$) and 1680 MeV ($I=\frac{1}{2}, J=\frac{5}{2}$). In the extended isobar model of Lindenbaum and Sternheimer,¹⁸ pion production is assumed to occur through the initial excitation of a nucleon to a state N^* , corresponding to one of these resonances, with subsequent emission of one or more pions, according to the reaction



where π_r is the recoil pion and π_d is the decay pion. Multiple-pion production, on the model, involves the initial formation of the higher mass isobars, followed by cascade decay through the $\frac{3}{2}, \frac{3}{2}$ state. The initial

¹⁴ T. J. Devlin, B. C. Barish, W. N. Hess, V. Perez-Mendez, and J. Solomon, *Phys. Rev. Letters* **4**, 242 (1960).

¹⁵ J. W. Cronin, *Phys. Rev.* **118**, 824 (1960).

¹⁶ C. D. Wood, T. J. Devlin, J. A. Helland, M. J. Longe, B. J. Moyer, and V. Perez-Mendez, *Phys. Rev. Letters* **6**, 481 (1961).

¹⁷ L. C. L. Yuan and S. J. Lindenbaum, in *Proceedings of the Fourth Annual Rochester Conference on High-Energy Nuclear Physics* (University of Rochester Press, Rochester, 1954), p. 99; H. C. Burrowes, D. O. Caldwell, D. H. Frisch, D. A. Hill, D. M. Ritson, R. A. Schluter, and M. A. Wahlig, *Phys. Rev. Letters* **2**, 119 (1959).

¹⁸ R. M. Sternheimer and S. J. Lindenbaum, *Phys. Rev.* **123**, 333 (1961).

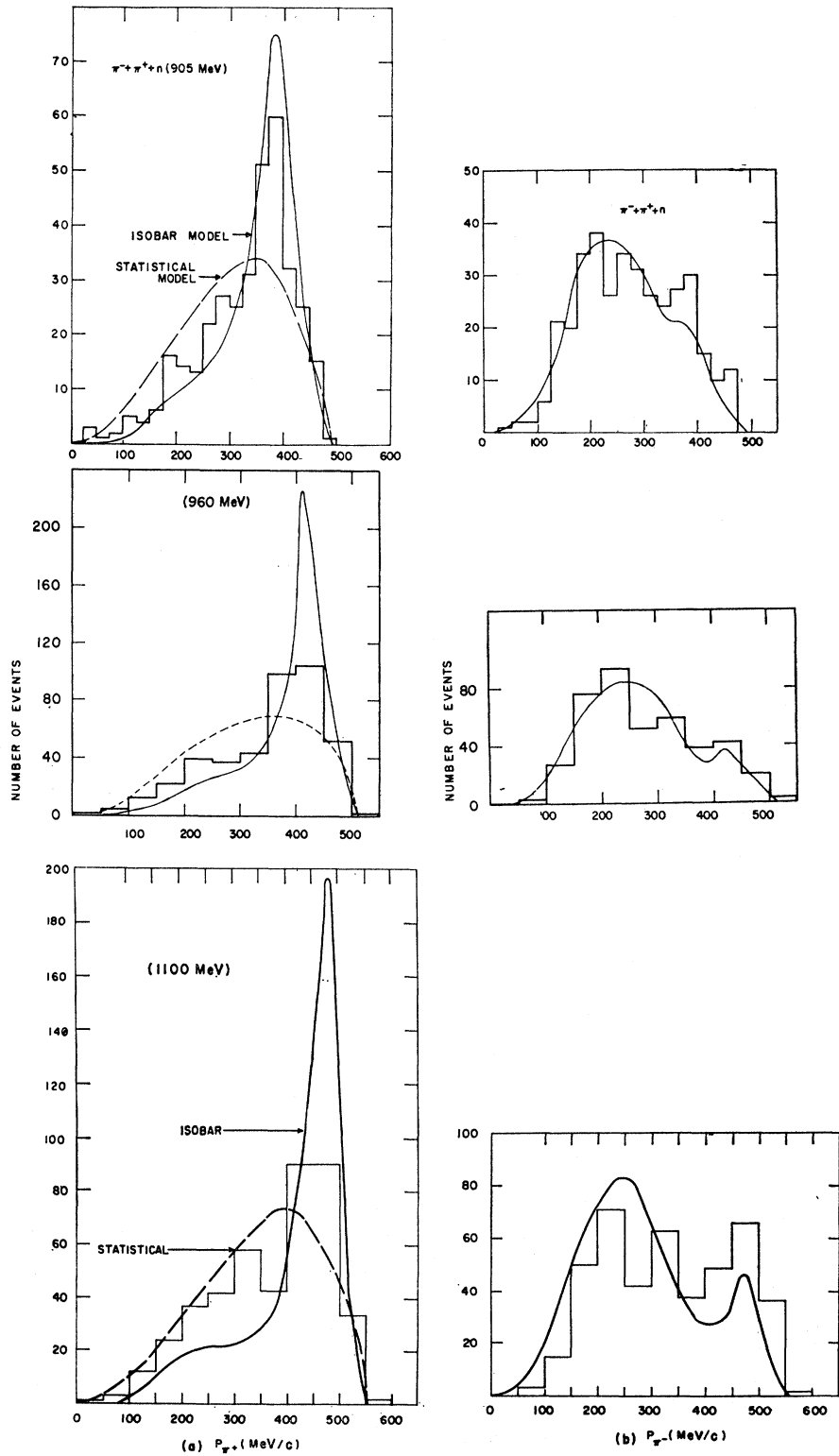


FIG. 2. Center-of-mass momentum distributions for (a) π^+ and (b) π^- from the reaction (1).

process is governed by two-body kinematics, so that the momentum distribution of the recoil pion must show peaking corresponding to the N^* mass and width.

The histograms in Fig. 2 show the c.m. momentum distribution of the positive and negative pions from reaction (1) for the three energies. Figure 3 shows

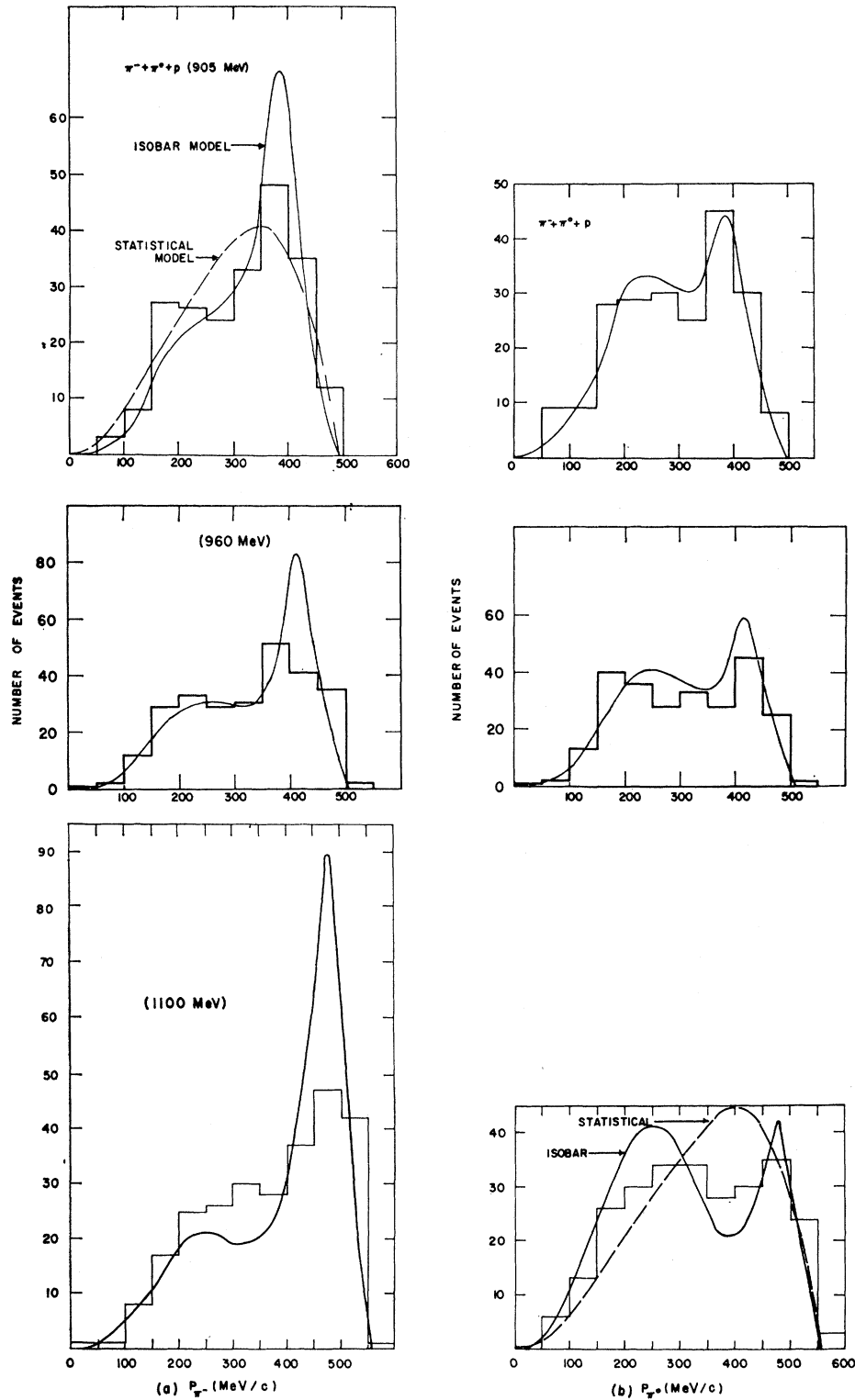


FIG. 3. Center-of-mass momentum distributions for (a) π^- and (b) π^0 from the reaction (2).

similar distributions for the neutral and negative pions from reaction (2). The dashed-line curves give the predictions of statistical theory, and the solid-line

curves the predictions of the extended isobar model. These were calculated according to the prescription given by Lindenbaum and Sternheimer.¹⁸ Our own

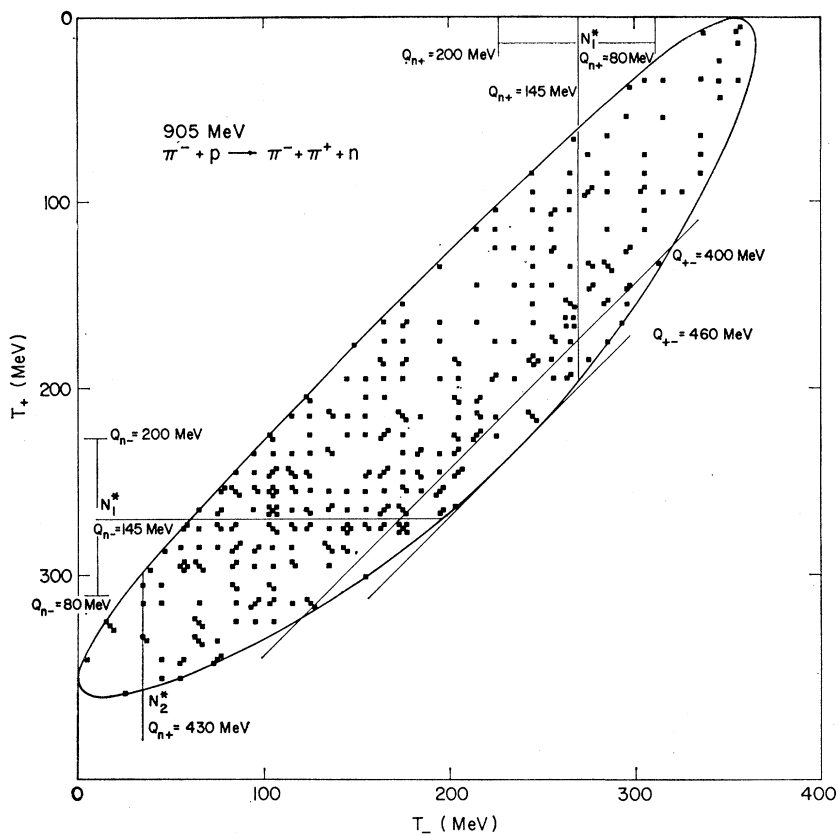
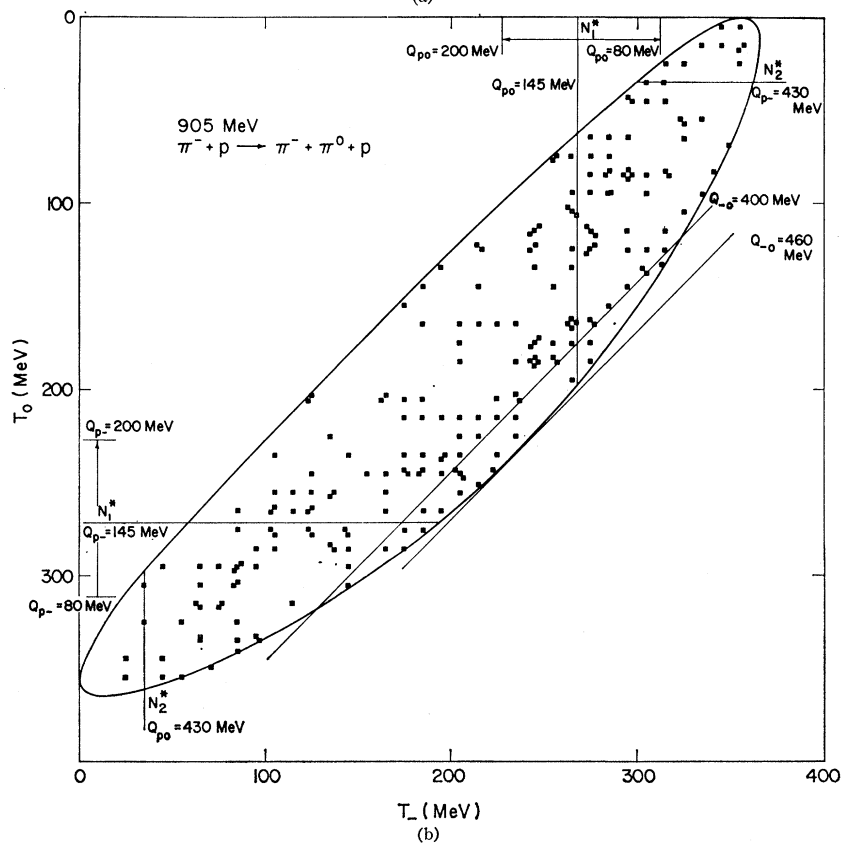


FIG. 4. Dalitz plots of the 905-MeV data, (a) reaction (1) and (b) reaction (2). The straight lines parallel to the axes indicate the expected positions of the 3,3 isobars. The diagonal lines indicate the region of the low-energy half of the ρ resonance.



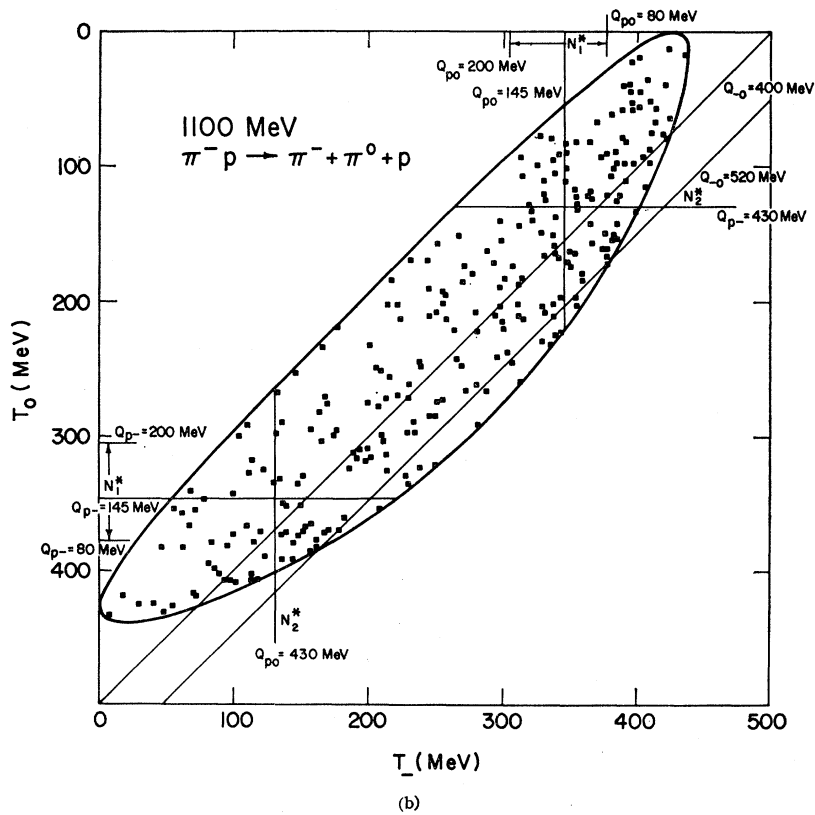
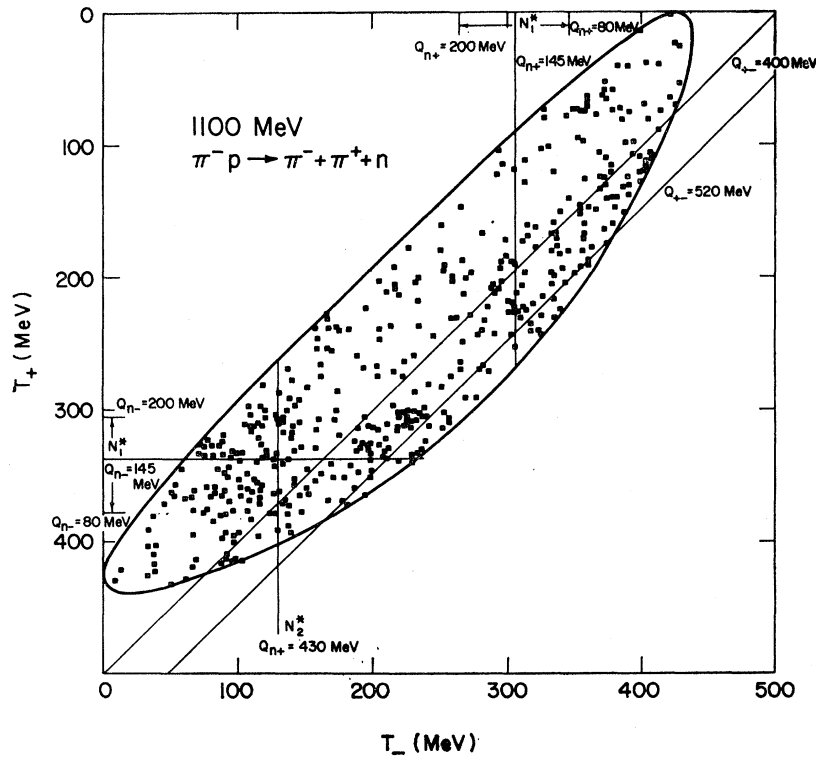


FIG. 5. Dalitz plots of the 1100-MeV data (a) reaction (1) and (b) reaction (2). The expected positions of the lower $I = \frac{1}{2}$ isobars are indications as well as the positions of the $I = \frac{3}{2}$ isobar. Note the strong overlap between the two isospin states. The diagonal lines indicate the full width (Γ) of the ρ meson.

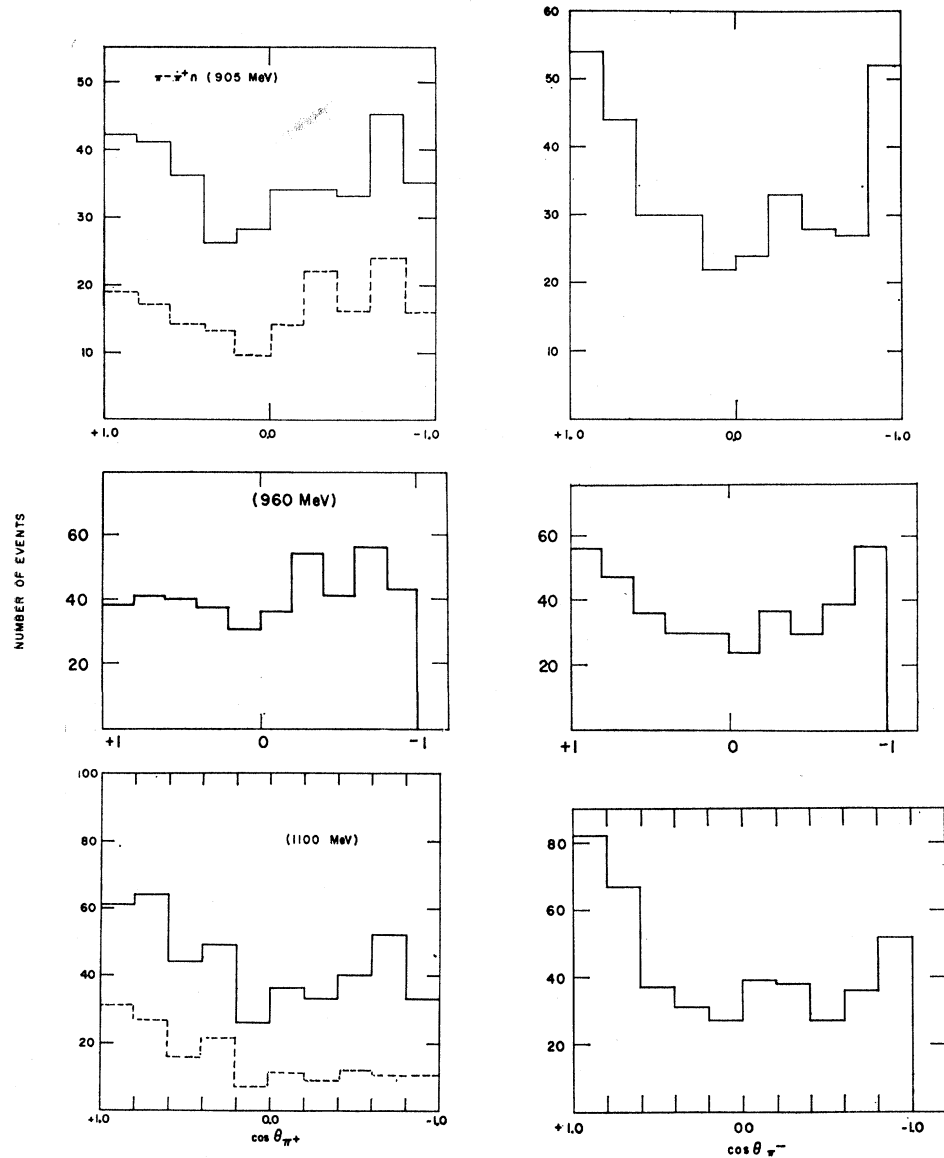


FIG. 6. Center-of-mass angular distributions of the pions from reaction (1). The dashed lines show those events which are consistent with production of the $n\pi^-$ isobar ($80 \leq Q_{n\pi^-} < 200$ MeV).

cross sections and the Yale $\pi^+ - p$ cross sections⁷ were used to obtain the partial cross sections for the various $I = \frac{1}{2}$ and $I = \frac{3}{2}$ isobar states.

The dominant peak in the experimental spectrum of π^+ from reaction (1) and π^- from reaction (2) due to the recoil pion produced with the $\frac{3}{2}, \frac{3}{2}$ isobar is evident at all three energies. There is no noticeable influence of the $I = \frac{1}{2}$ isobars, but at these energies the recoil pions from the higher states would be masked by decay pions from the $\frac{3}{2}$ state; the regions of $I = \frac{1}{2}$ and $I = \frac{3}{2}$ resonances are indicated in the Dalitz plots for the 905- and 1100-MeV experiments (see Figs. 4 and 5).

At 905 MeV the agreement between experiment and the isobar calculation is fairly good for reaction (1), but less satisfactory for reaction (2). The agreement becomes progressively poorer at the higher energies,

thus indicating the increasing importance of processes not included in the extended isobar model, such as interactions between final-state particles or peripheral pion-pion interactions.

B. Pion Angular Distributions

Figures 6 and 7 show the c.m. angular distributions of the pions from the two reactions. The dashed-line histograms for 905 and 1100 MeV show the distributions for events with $80 \leq Q_{n\pi^-} < 200$ MeV, corresponding to recoil pions from the dominant $n\pi^-$ isobar. At 905 MeV the $n\pi^-$ isobar is produced approximately isotropically in the c.m. system (see the π^+ distribution, Fig. 6). At 1100 MeV there appears to be some asymmetry. However, it is impossible to tell if this asymmetry in the pion

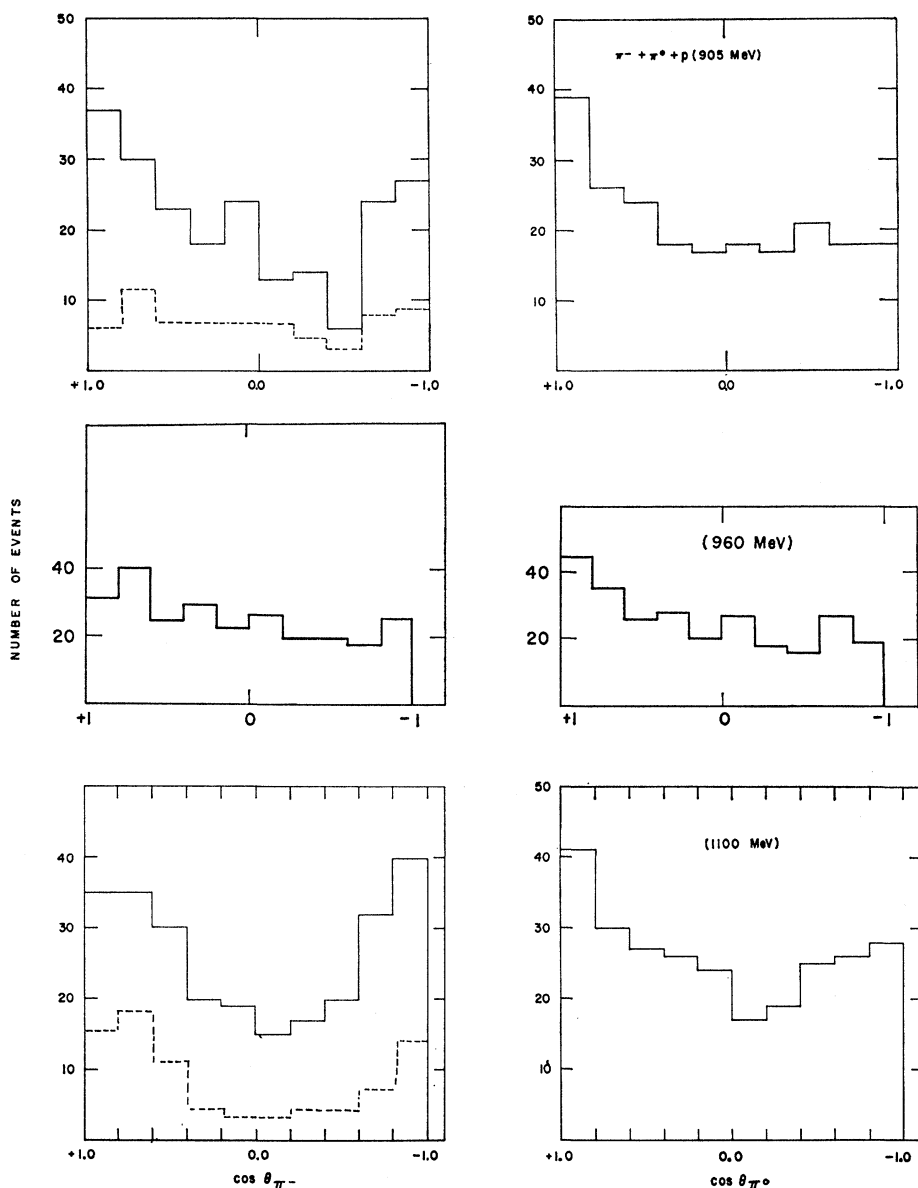


FIG. 7. Center-of-mass angular distributions of the pions from reaction (2). The dashed lines show those events with $(80 \leq Q_{p\pi^0} < 200 \text{ MeV})$.

angular distribution is to be associated with a change in isobar production angle or with the other interactions known to be present (for example, $\pi\pi$ interactions). A similar ambiguity applies to the $p\pi^0$ isobar at both energies since the momentum distributions exhibit departure from the isobar picture even at 905 MeV.

C. $\pi\pi$ Q -Distributions

Figures 8 and 9 show histograms of the $\pi^+\pi^-$ and $\pi^-\pi^0$ distributions for the three energies, with the predictions of the statistical model. The Lindenbaum-Sternheimer isobar model gives similar predictions. The distributions at 905 MeV show peaks at the high-energy end of the spectra which are consistent with some slight influence

of the ρ resonance. Poor resolution may have weakened the peaks at 960 MeV although, as reported previously,⁴ there is indication of the ρ in those events in which the nucleon is emitted backward in the center-of-mass system (low four-momentum transfer collisions). At these energies phase space limitations cause an apparent shift of the peak to a lower mass. At 1100 MeV the experimental distributions clearly show the effect of the ρ resonance in both the $\pi^+\pi^-$ and $\pi^-\pi^0$ systems.

There is no indication of a resonance in the region $Q \sim 300 \text{ MeV}$ (ζ) for either the neutral or the charged $\pi\pi$ state, nor does a separation of the events into high- and low-momentum transfer reveal an effect associated with either group. Such a resonance would probably be most apparent in the 905-MeV experiment. The

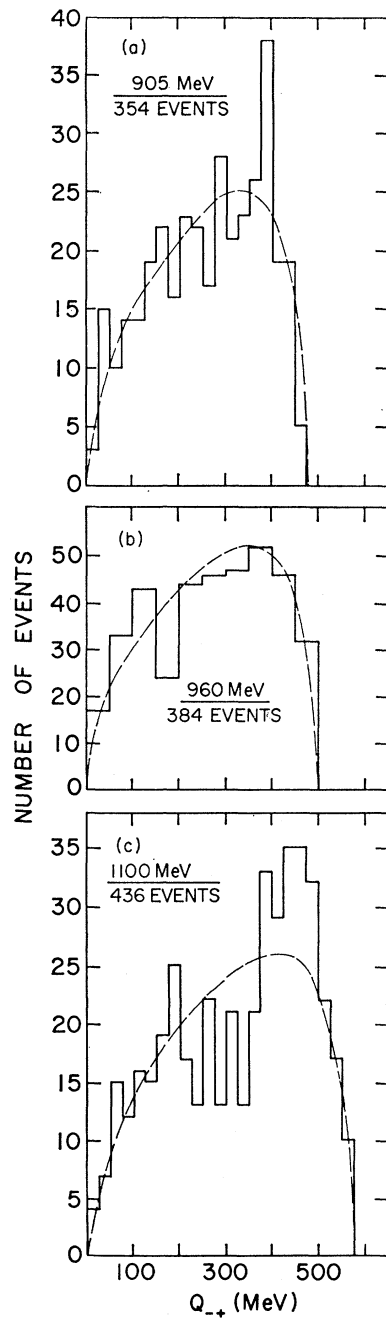


FIG. 8. Distributions of Q_{-+} . The curves show the predictions of the statistical model normalized to the total number of events in each histogram.

absence of any effect is consistent with the Yale results¹⁹ but inconsistent with those of Saclay²⁰ for the $\pi^+\pi^0$ system. While the possibility of an $I=1$ resonant state in the region $Q \sim 300$ MeV cannot be excluded, the data available at present seem to be consistent with the influence of just one resonant state, the ρ .

¹⁹ D. L. Stonehill and H. L. Kraybill, Rev. Mod. Phys. **34**, 503 (1962).

²⁰ R. Barloutaud, J. Heughebaert, A. Leveque, C. Louedec, J. Meyer, and D. Tycho, Nuovo Cimento **27**, 238 (1963).

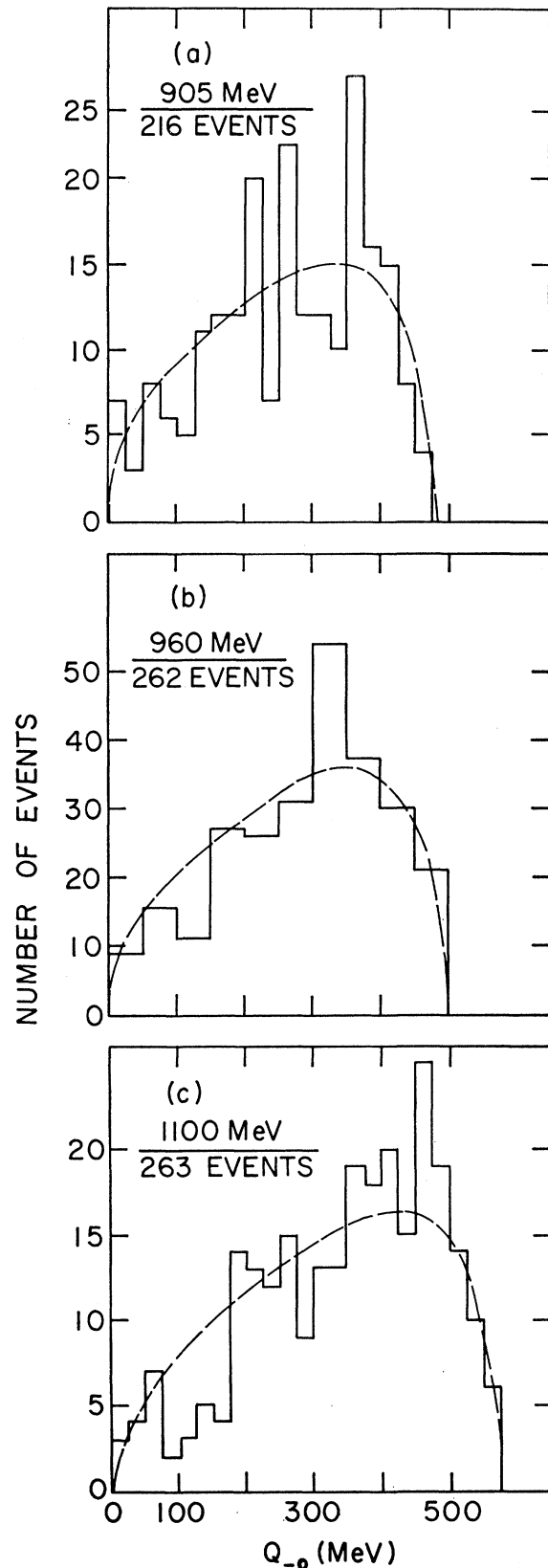


FIG. 9. Distributions of Q_{-0} with predictions of the statistical model.

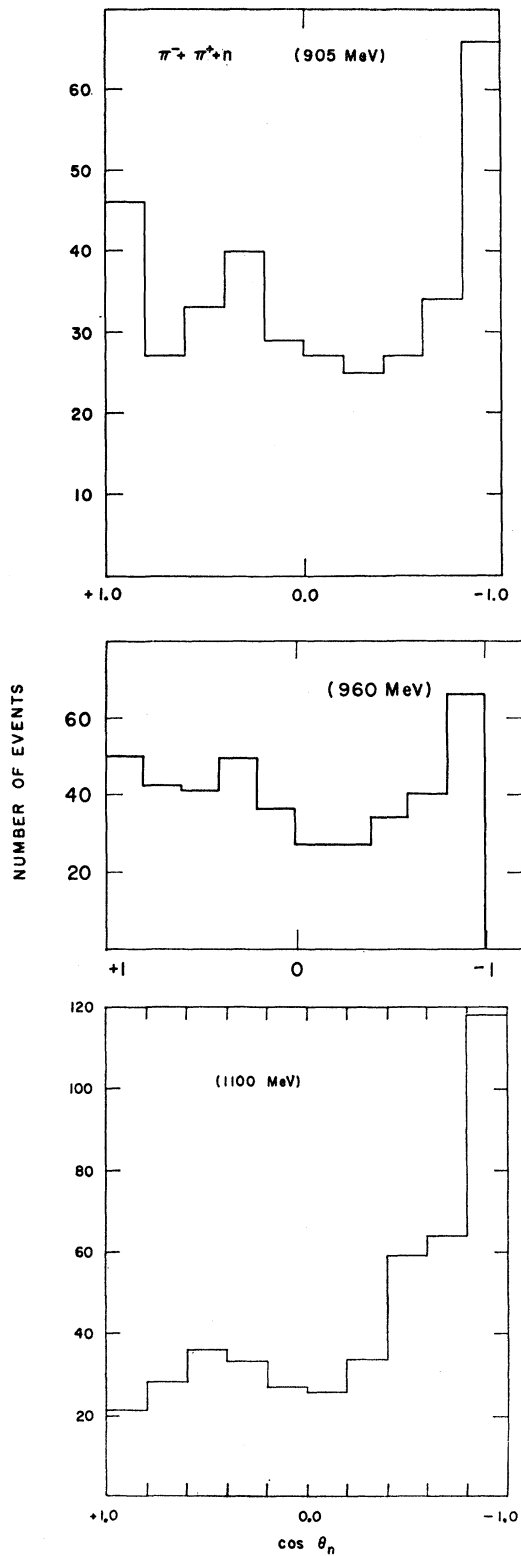


FIG. 10. Center-of-mass angular distributions of the neutrons from reaction (1).

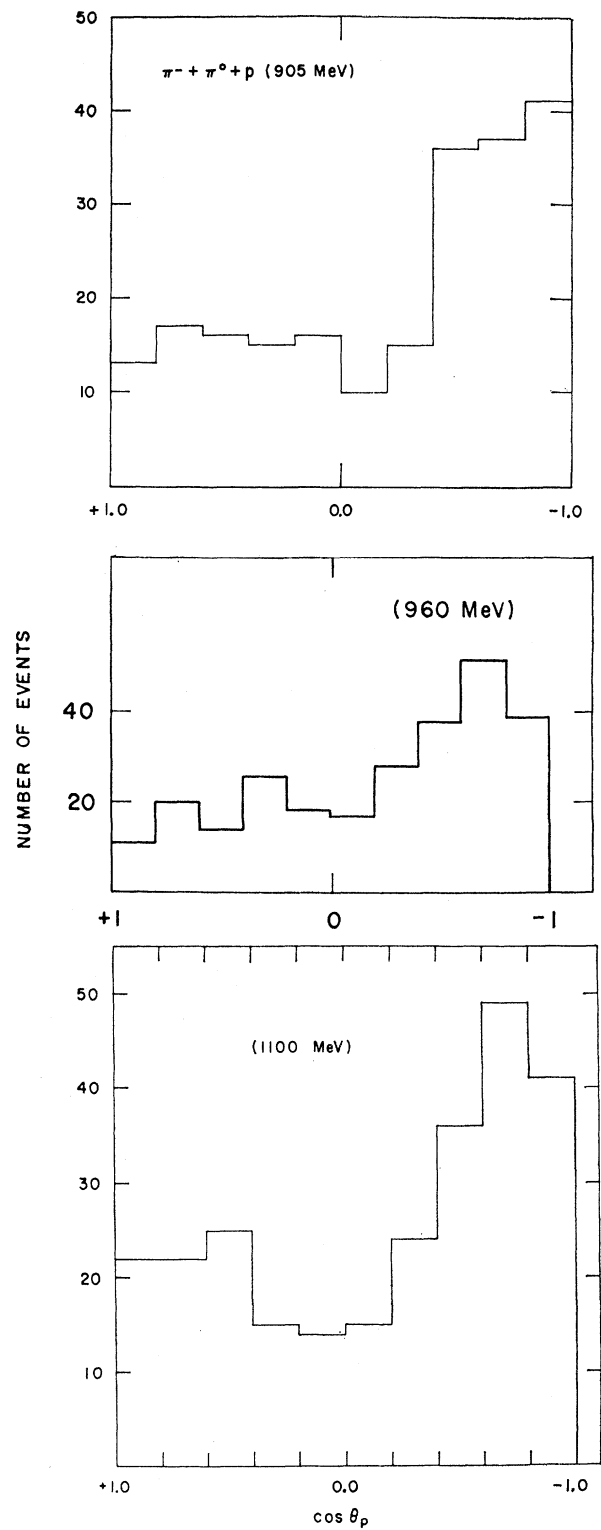


FIG. 11. Center-of-mass angular distributions of the protons from reaction (2).

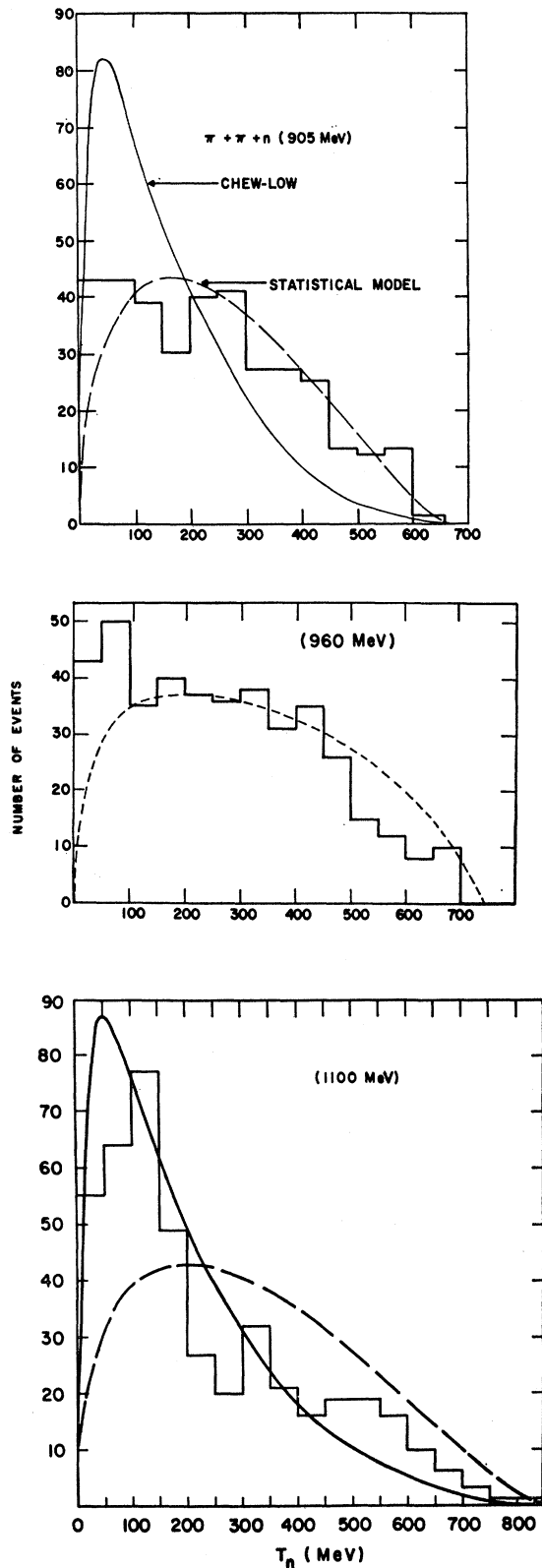


FIG. 12. Laboratory kinetic energy (T_n) distributions of the neutrons from reaction (1).

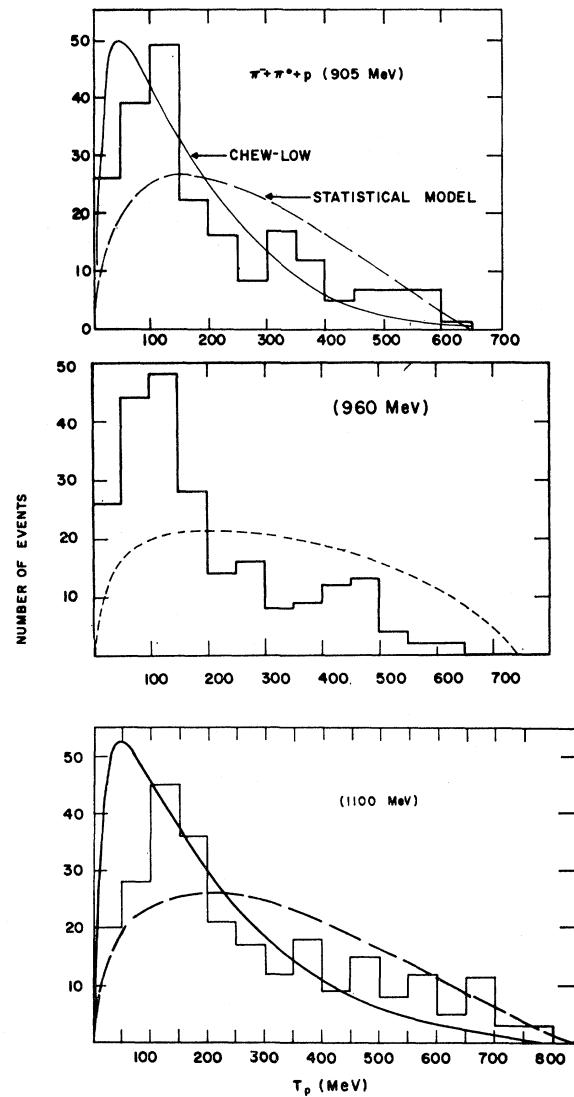


FIG. 13. Laboratory kinetic energy (T_p) distributions of the protons from reaction (2).

D. C.M. Angular Distributions and Laboratory Kinetic Energy Distributions of the Nucleons

Figures 10 and 11 show the c.m. angular distributions of the final-state nucleons from reactions (1) and (2). At 905 and 960 MeV the neutron distributions are almost symmetric about 90° , but the proton distributions are predominately backward; at 1100 MeV both neutrons and protons are produced predominately backward in the c.m. system.

The latter distributions strongly suggest peripheral collisions; such collisions are a characteristic of the one pion exchange (OPE) interaction. In the OPE model, single-pion production occurs through elastic scattering of the incident pion by a virtual pion in the peripheral

cloud of the nucleon, with small momentum transfer to the recoil nucleon.

Figures 12 and 13 show the distributions of the nucleon laboratory kinetic energy (T), which is proportional to the square of the four-momentum transfer to the nucleon ($\Delta^2 \simeq 2MT$). Low-energy peaking of the protons at all three incident energies, and of the neutrons at 1100 MeV is observed, corresponding to the asymmetric angular distributions.

The dashed-line curves in Figs. 12 and 13 show the predictions of the statistical model; the predictions of the Lindenbaum-Sternheimer isobar model are similar if it is assumed that the isobar is produced isotropically in the center-of-mass system. The solid curves show the predictions of the OPE model [$\sim \Delta^2 / (\Delta^2 + m_\pi^2)^2$], normalized to the experimental data.

The low-energy peaking of the neutrons and protons at 1100 MeV is in reasonable qualitative agreement with the OPE curve. Exact agreement over the entire range of T is not expected since non-OPE processes also occur, particularly at high-momentum transfers. It may be noted that at 1100 MeV there is still considerable 3,3 isobar production which cannot be formed by the OPE process in reactions (1) and (2). At higher incident energies, where cleaner separation of the ρ from competing processes is possible, it has been observed²¹ that an unmodified OPE model is inadequate to describe ρ production. Selleri²² has suggested introduction of a pion form factor into the OPE calculations to bring about better agreement between experiment and theory.

The nucleon laboratory kinetic energy distributions at 905 and 960 MeV are more difficult to interpret. At these energies it is possible to excite the first $I = \frac{1}{2} \pi^- - p$ resonance as well as the 3,3 isobar, and in addition 905 MeV is close to the peak of the second $I = \frac{1}{2}$ resonance and the threshold for exciting the center of the ρ resonance. These energies thus are in a region of transition between relatively simple 3,3 isobar formation and more complex processes. It is possible that interference effects among these various states may account for the differences between the laboratory kinetic energy

distributions of the protons and neutrons at 905 and 960 MeV.

The proton distributions are, however, strongly suggestive of peripheral interactions, and it is tempting to try to explain them in terms of OPE. Since the ρ is an $I = 1$ state, its influence should be stronger in the neutron than in the proton events [$(\sigma_{-0}/\sigma_{+-})_{I=1} = \frac{1}{2}$]. An $I = 2 \pi^- - \pi$ interaction would affect more strongly the proton events than the neutron events [$(\sigma_{-0}/\sigma_{+-})_{I=2} = \frac{3}{2}$]. The experimental distributions are thus consistent with formation of the 3,3 isobar plus an $I = 2$ pion-pion interaction.

The existence of an $I = 2$ pion-pion interaction has been suggested by the asymmetries in angular distributions of $\pi^- \pi^0$ and $\pi^+ \pi^0$ scattering above and below the ρ resonance, observed by the Berkeley group²³ and by the Saclay-Orsay-Bari-Bologna collaboration.²¹ Further evidence for this state has been found by Barloutaud *et al.*²⁰ in the ratio of cross sections for π^+ and π^0 production in $\pi^+ p$ interactions at energies similar to ours.

IV. CONCLUSIONS

The main features of single-pion production in $\pi^- - p$ collisions in the 1 BeV region can be explained in terms of (1) 3,3 isobar formation; (2) the $I = 1 \pi\pi$ resonance (ρ) at ~ 750 MeV; (3) a nonresonant $I = 2 \pi\pi$ interaction.

At 905 MeV the $\frac{3}{2}, \frac{3}{2}$ isobar dominates single-pion production. C.m. angular distributions and laboratory kinetic energy distributions of the nucleons suggest that there is some $I = 2 \pi\pi$ interaction. There is also a peaking at the upper end of the $\pi\pi Q$ distributions consistent with off-peak excitation to the ρ resonance. As the energy is increased through 960 to 1100 MeV the ρ resonance begins to replace the isobar as the dominant feature.

ACKNOWLEDGMENT

We wish to thank the BNL Bubble Chamber Group, the members of the Cosmotron staff, and our scanners for their invaluable services. We also wish to thank Dr. R. M. Sternheimer for helpful discussions.

²¹ Saclay-Orsay-Bari-Bologna collaboration, *Nuovo Cimento* **25**, 365 (1962).

²² F. Selleri, *Phys. Letters* **3**, 76 (1962).

²³ D. D. Carmony and R. T. Van de Walle, *Phys. Rev. Letters* **8**, 73 (1962).